

# OPTIMIZATION OF A GRID-INTERACTIVE BUILDING ENERGY SYSTEM CONSIDERING USER SATISFACTION

Yizhuo Zhang, Tori Wiederhöft, Thomas Schreiber, and Dirk Müller

RWTH Aachen University, E.ON Energy Research Center, Institute for Energy Efficient Buildings and Indoor Climate Aachen, Deutschland, E-Mail: [yizhuo.zhang@eonerc.rwth-aachen.de](mailto:yizhuo.zhang@eonerc.rwth-aachen.de)

## Abstract

Grid-interactive building energy systems (BES) enable the transition of buildings to flexible energy consumers. Nonetheless, occupant satisfaction, which is relevant for the spread of the technology, plays a subordinate role compared to costs in the research works on the grid-interactive BES operation. This work proposes a mixed-integer linear program (MILP) to integrate user aspects concerning thermal comfort and electric vehicle (EV) charging preferences in grid-interactive strategies. Applying the method to a single-family house shows that the simultaneous optimization of thermal comfort and costs is promising for the application scenario of the grid-interactive BES operation. Further, we demonstrate efficient integration strategies for EV charging scheduling.

## Introduction

The rising share of fluctuating renewable energy sources and the ongoing electrification of heating and mobility sectors increase the demand for flexibility and grid-interactive technology to ensure a stable power supply (Bründlinger et al., 2018). Making buildings more flexible can lead to dissatisfaction, as energy is no longer drawn only when needed but also when available. Thus, considering user preferences in energy consumption could help achieve high user satisfaction and improve technology acceptance. Different studies work on intelligent grid-interactive methods but not or only partly consider user perspectives (Yong et al., 2015, Ascione et al., 2016, Korkas et al., 2016)

This work proposes methods to comprehensively consider thermal comfort and EV charging preferences and integrate the user perspectives into the grid-interactive operation strategies. We develop a MILP to simulate nine different operation strategies and apply them to a use case - a single-family house with a fully electrified BES. By comparing operation strategies according to specific metrics, we offer suggestions to promote the grid-interactive technology in residential buildings.

## Proposed method

In this section, we propose approaches to evaluating thermal comfort and considering user preferences

concerning EV charging in a residential building, and integrating these user aspects into BES operation strategies. First, we present the basic BES optimization model with an integrated simplified thermal building model to simulate operation strategies without considering various user preferences. Second, we illustrate the optimization objectives based on the predicted mean vote (PMV) to implement operation strategies considering thermal comfort. Third, we introduce the implementation of three EV charging strategies by modifying the constraints in the MILP model. The charging strategies represent three user types with varying charging preferences. At last, we present two flexibility indicators to assess the grid supportive effects of the studied operation strategies.

## Model formulation

The BES of the studied single-family house comprises an air-to-water heat pump (HP) and an electric heater (EH) covering the demand for space heating and domestic hot water, a photovoltaic system (PV), a thermal storage system (TES), and a battery (BAT) offering flexibility for the BES. The PV can feed electricity back to the local distribution grid (DG), which the DG operator compensates. Besides, an EV with bidirectional charging can be an additional electricity storage unit. In the discharging mode, the electricity from the EV can either be used to meet the electricity demand (Vehicle-to-home/V2h) or be fed back into the power grid (Vehicle-to-grid/V2G). Figure 1 shows the schematic representation of the considered BES.

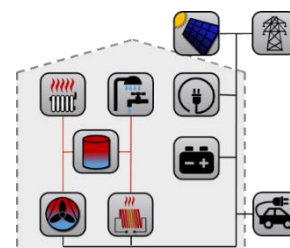


Figure 1: The investigated building energy system

We apply a MILP with different optimization objectives and constraints to simulate various operation strategies, particularly for the consideration of various user aspects. The optimization model of this work evolves from a design operation model of Thomas Schuetz (Schütz et al., 2017). We modified

the original model, which was based on design days, to simulate the operation of BES in a year (365 days with 24 hours per day). All components are constrained with boundary conditions representing their physical behavior—for example, minimum and maximum power of the electricity consumption and generation devices. The model considers the hourly demand for space heating ( $\dot{Q}_{d,t}^{SH}$ ), domestic hot water, and hourly electricity demand for plug loads and EV charging ( $P_{ch,d,t}^{EV}$ ). The thermal and electricity balance between the demand and supply units of BES in each timestep are formulated as constraints in the model.

To evaluate the thermal comfort, which is primarily dependent on room temperatures, we employ the simplified thermal building model (5R1C model) based on DIN EN ISO 13790, which formulates the thermal energy balance of the building with linear equations for each hour while considering the internal gains, solar gains, and heat transfer from ventilation and transmission (DIN e. V., 2008). The 5R1C model lumps all zone components (like the roof and outer walls) into one thermal mass with capacitance  $C_m$  and area  $A_m$ . Besides, three nodes model the indoor air temperature  $\theta_{d,t}^{air}$ , the thermal capacitance's surface temperature  $\theta_{d,t}^s$ , and mass temperature  $\theta_{d,t}^m$ , which is a mix of indoor air and mean radiation temperature.

The 5R1C model is intended to calculate sensible energy for space heating and cooling. Meanwhile, the room temperatures from this model can be potentially used to evaluate thermal comfort, which has been implemented in previous works (Michalak, 2022). In addition, the measurements in (Csáky & Kalmár, 2015) prove the 5R1C model to provide appropriate indoor air temperature values. In (Michalak, 2022), the results for a residential building indicate a strong correlation between the operative temperature (a weighted average of the air and the mean radiation temperature) from the 5R1C model and the detailed simulations in the EnergyPlus program. Thus, we assume that the mean radiation temperature from 5R1C can be used to calculate PMV and assess thermal comfort. This assumption, though, should be validated in further field measurements.

We model the studied single-family house as a single-zone building and integrate it into the MILP model to calculate the  $\dot{Q}_{d,t}^{SH}$  and room temperatures. The relevant constraints determining their values are a given PMV range and the thermal energy balance of BES and the building. Like domestic hot water and plug loads, the other demands are provided as fixed time-series inputs. For EV, the daily electricity demand is given. Besides, we define the daily parking period of EV at home by arrival time ( $t_d^{arr}$ ) in the evening and departure time ( $t_{d+1}^{dep}$ ) the following day.

In the basic model, without consideration and evaluation of thermal comfort, the optimization objective is to minimize total electricity costs in a year ( $c^{tot}$ ) while taking the remuneration from PV feed-in ( $P_{d,t}^{f-in}$ ) with a fixed remuneration rate ( $p^{f-in,PV} = 9.72 \text{ €ct/kWh}$ ) into account. Thus, the objective function is altered to

$$\min c^{tot} = c^{DG,el} - r^{f-in,PV} \quad (1)$$

$$c^{DG,el} = \sum_{d=1}^{365} \sum_{t=1}^{24} (P_{d,t}^{DG} * p_{d,t}^{el}) \quad (2)$$

$$r^{f-in,PV} = p^{f-in,PV} * \sum_{d=1}^{365} \sum_{t=1}^{24} P_{d,t}^{f-in} \quad (3)$$

$c^{DG,el}$  is the yearly costs because of the utilization of electricity from DG;  $P_{d,t}^{DG}$  is the electric power from DG in each timestep;  $p_{d,t}^{el}$  is the electricity rate at the hour  $t$  on the day  $d$ ,  $\text{€ct/kWh}$ . The flexibility of the BES operation is dependent on the variety of the electricity prices. We employ in this work a tariff from aWATTar (aWATTar, 2021) with hourly variable supply rates.

#### PMV-based thermal comfort quantification

To integrate thermal comfort in the operation strategy, we define two optimization objectives in Equation 4, maximizing the yearly thermal satisfaction level (TSL), and Equation 5, minimizing the electricity costs per TSL:

$$\max TSL = \frac{1}{24 * 365} * \sum_{d=1}^{365} \sum_{t=1}^{24} TSL_{d,t} \quad (4)$$

$$\min J = \frac{c^{tot}}{TSL} \quad (5)$$

The former describes the user type pursuing maximum thermal comfort, while the latter demonstrates the heating behavior resulting from a trade-off between thermal comfort and energy costs.  $TSL$  represents the average user satisfaction concerning thermal comfort in each timestep ( $TSL_{d,t}$ ) in a year. To quantify the thermal comfort, we employ in this work the PMV from DIN EN ISO 7730 (DIN e. V., 2006).

PMV is an established metric to predict the mean thermal sensation vote of a group of occupants (Ascione et al., 2016). Evaluated in the PMV model is the heat balance of occupants under consideration of air temperature, mean radiation temperature, airspeed, humidity, metabolic rate, and clothing insulation. Although this heat balance approach was developed from laboratory studies, it has considerable flexibility and broad applicability and has been applied throughout every type of building in the field research (van Hoof, 2008). While PMV represents the average

comfort of all occupants, various studies take PMV or the Predicted Percentage of Dissatisfied people (PPD), which is calculated from PMV, as a part of the optimization objective to integrate the thermal comfort optimization in the BES operation simulation (Korkas et al., 2016, Samadi et al., 2020). Another conventional methodology to quantify the thermal comfort determines the deviation from a temperature or a temperature range assumed to be optimal, such as the comfort temperature range from the adaptive thermal comfort model in DIN EN 15251 (DIN e. V., 2012). The application of this model is restricted to naturally ventilated buildings and is not implemented in this work. A comparison of the PMV and adaptive thermal model for thermal comfort optimization could be a focus of future works.

Regarding the linear optimization problem in this work, we adopt the method introduced by Jiří Cigler et al. (Cigler et al., 2012) with proven high accuracy to linearize the original nonlinear equations in DIN EN ISO 7730 to calculate PMV. Besides, we consider an airspeed of 0.05 m/s in winter and 0.17 m/s in summer and a constant humidity of 50 %, based on measurements in (Oreszczyn et al., 2006, Yang & Zhang, 2009). To take the adaptive behavior into account and for more realistic results, we consider the variations of dressing and activity over the day and seasons to determine the clothing insulation and metabolic rate profile.

With the linearization and the assumptions mentioned above, we formulate the PMV as a linear function of room air temperature and mean radiation temperature from the 5R1C model. Based on the results published in (Rupp et al., 2015), we modify the boundaries of PMV to be between -1 (slightly cool) and 1 (slightly warm) to ensure primary comfort conditions at each timestep and choose 1 as the reference value ( $PMV^{max}=1$ ) for the calculation of  $TSL_{d,t}$  with Equation 6.

$$TSL_{d,t} = 1 - occ_{d,t} * \frac{|PMV_{d,t}|}{PMV^{max}} \quad (6)$$

$occ_{d,t}$  equals one if at least one person is at home; otherwise, zero. In the studied household, we assume a maximum of three occupants and adopt the occupant profile of the single-family house in (Schweizerischer Ingenieur- und Architektenverein (SIA), 2015).

### Modeling of EV charging strategies

Charging behavior is dependent on the user preferences regarding EV charging, which should be a trade-off between mobility flexibility and financial benefits (Zhang et al., 2020). In particular, decisions about EV charging strategies result from an overall consideration of the state of charge (SoC) of the EV battery at the time of use, time of complete charging,

and charging costs (Daina et al., 2017). In general, charging behaviors can be divided into economic and urgent drivers. For the former, the time of finished charging is irrelevant as long as the SoC of the battery at the desired time reaches a given minimum (Mohsenian-Rad et al., 2010). For the latter, the EV drivers prefer rapid charging in case of unexpected vehicle use before the planned departure (Daina et al., 2017). Based on these two EV driver types, we implement two charging strategies by modifying the EV charging constraints in this work: flexible charging (FC) and rapid charging (RC). Besides, we assume a compromised charging (CC) behavior that pursues a possibly fast charging, while the charging expenses should be as low as possible.

One of the common constraints of the three strategies is that the EV should be fully charged one hour before the departure to take the uncertainty about departure time into account and to avoid range anxiety for not experienced drivers (Rauh et al., 2015). Three charging strategies differ mainly in the charging time, charging power, and discharging possibility. The relevant constraints are demonstrated in Table 1.

Table 1: EV charging strategies

Charging strategy	Flexible charging (FC)	Compromised charging (CC)	Rapid charging (RC).
Charging time	At any time between arrival and departure the next day	In possibly early hours with low electricity rates.	Immediately after arriving home
Charging power	Any value between zero and the maximum ( $P_{ch,max}^{EV}$ )	Possibly with the full power to ensure a short charging duration.	
Discharging allowed	Yes: $P_{dch,d,t}^{EV} \geq 0$	No: $P_{dch,d,t}^{EV} = 0$	

For charging strategy CC, we introduce a metric, the  $score_{d,t}^{EV}$ , to evaluate each hour between arrival and departure and determine the charging hours in the preprocessing. The  $score_{d,t}^{EV}$  results from a combined evaluation of financial benefits ( $score_{d,t}^{financ}$ ) and mobility flexibility ( $score_{d,t}^{flex} = t - t_d^{arr}$ ) with Equation 7. The constant  $c$  in Equation 8 normalizes the charging costs so that the time  $t - 1$  (one hour

earlier than  $t$ ) and time  $t$  with  $c$  € lower charging fees ( $P_{ch,max}^{EV} * p_{d,t-1}^{el,tar} - P_{ch,max}^{EV} * p_{d,t}^{el,tar} = c$ ) have the same score. The value of  $c$  represents the equivalent additional costs per hour later charging and can be used to define different user types.

$$score_{d,t}^{EV} = score_{d,t}^{financ} + score_{d,t}^{flex} \quad (7)$$

$$score_{d,t}^{financ} = \frac{P_{ch,max}^{EV} * p_{d,t}^{el}}{c} \quad (8)$$

For each day between arrival and departure, we calculate  $score_{d,t}^{EV}$  and sort the values in descending order. The charging duration under  $P_{ch,max}^{EV}$  is determined and rounded into the higher integer value  $n_d$ . In the *CC* strategy, the EV will be charged in the  $n_d$  hours with the lowest  $score_{d,t}^{EV}$ .

Under one of the introduced optimization objectives and the constraints of an implemented EV charging strategy, the MILP model can calculate the profiles of the SoC of the EV battery. To evaluate the satisfaction of the EV user type that tends to avoid risks of unanticipated vehicle use and thus prefers rapid charging, we calculate the user satisfaction ( $EVSL_d$ ) for each day with Equation 9 and the average EV user satisfaction in a year ( $EVSL$ ) based on  $EVSL_d$  with Equation 10.

$$EVSL_d = 1 - \frac{D_d^{full} - D_d^{full,min}}{t_d^{latest,full} - t_d^{earliest,full}} \quad (9)$$

$$EVSL = \frac{1}{365} * \sum_{d=1}^{365} EVSL_d \quad (10)$$

$D_d^{full}$  is the distance of complete charging to the arrival time, deriving from the SoC profiles. As references, we assume that urgent users are most satisfied if the EV is charged uninterrupted in the first  $n_d$  hours after arriving home. This charging preference results in the earliest fully charging time  $t_d^{earliest,full}$ , and  $D_d^{full,min}$  is its distance to arrival time. In the case with the lowest user satisfaction, the EV doesn't complete the charging until one hours before departure ( $t_d^{latest,full} = t_d^{dep} - 1$ ).

### Indicators of BES flexibility

Different studies have developed a series of indicators to evaluate the BES flexibility and the resulting grid-supportive effects (Jaume Salom et al., 2011, Verbruggen & Driesen, 2015). We employ in this work two of them: No-Grid Interaction Probability (NGIP) and One-Percent Peak Power (OPP).

The NGIP exhibits the probability that the building is acting autonomously of the grid and is altered to Equation 11 (Jaume Salom et al., 2011).

$$P_{E \approx 0} = \frac{time_{|E(t)| < 0.001}}{T} \quad (11)$$

The OPP (Eq. 12) represents the average exchange power between the DG and BES in the 1% peaks in a time interval ( $T$ ). By comparing it with the house connection capacity ( $\frac{OPP}{P_{cap}}$ ), the  $OPP_{cap}$  is determined.

The  $OPP_{cap}$  represents peak house connection capacity utilization. (Verbruggen & Driesen, 2015) In the following, we consider only  $OPP_{cap}$ .

$$OPP = \frac{E_{1\% peak}}{T/100} \quad (12)$$

## Analysis and discussion of the results

We apply the developed model to a typical single-family house according to (Bundesministerium für Verkehr, Bau und Stadtentwicklung, 2007) with a construction year between 1969 and 1978, light construction, and the same geometry as the building in (Schütz et al., 2017). By variation of optimization objectives and constraints, we implement nine BES operation strategies and assess their performance in terms of electricity costs, TSL, EVSL, and flexibility. Table 2 shows the overview of model settings in the studied scenarios.

Table 2: Optimization scenarios

Scenario	Optimization objective	EV charging strategy
<i>C+FC</i>	$\min c^{tot}$	<i>FC</i>
<i>C+CC</i>	$\min c^{tot}$	<i>CC</i>
<i>C+RC</i>	$\min c^{tot}$	<i>RC</i>
<i>J+FC</i>	$\min J$	<i>FC</i>
<i>J+CC</i>	$\min J$	<i>CC</i>
<i>J+RC</i>	$\min J$	<i>RC</i>
<i>TSL+FC</i>	$\max TSL$	<i>FC</i>
<i>TSL+CC</i>	$\max TSL$	<i>CC</i>
<i>TSL+RC</i>	$\max TSL$	<i>RC</i>

Figure 2 illustrates the electricity costs, TSL, and EVSL with  $c = 0.02$  €, and Figure 3 shows the results of BES flexibility evaluations in the nine scenarios. In Figure 3, we present the values of 1-OPP instead of OPP for a better-visualized comparison.

The first aspect of being recognized is that a sole optimization of TSL can significantly increase electricity costs (on average + 200 % compared with

other scenarios) while improving the TSL on a relatively smaller scale (on average + 17 %). Besides, in these scenarios, we observe a reduction in BES flexibility compared to other scenarios. Reaching the scenarios with the other two optimization objectives, we notice that  $\min J$  leads to higher TSL and NGIP than cost minimization, while their electricity costs and the values of 1-OPP are nearly the same (differences less than 2 %). Thus, the scenarios with  $\min J$  as the optimization objective, with low energy costs and appropriate TSL values, could be promising to promote the grid-interactive BES operation.

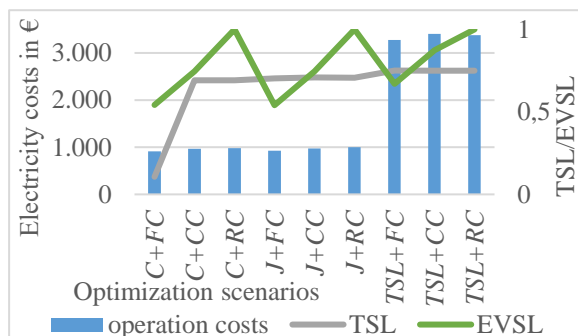


Figure 2: Electricity costs, TSL, and EVSL in different optimization scenarios

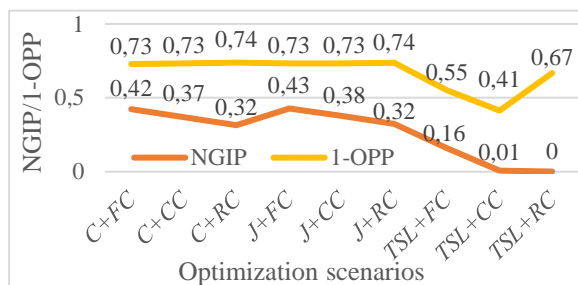


Figure 3: Grid related building performance in different optimization scenarios

Despite the lowest expenses and highest NGIP of the flexible charging strategy in most scenarios, it should not be promising for implementation in practice because its economic benefits compared with the rapid charging strategy are negligible. Besides, the rapid charging strategy shows higher BES flexibility with lower mean peak power (OPP) than the flexible and the introduced comprised charging strategy. Nevertheless, the introduced comprised variant (CC) has higher NGIP and lower charging expenses (except for the scenario with max TSL) than the uninterrupted charging. At the same time, its OPP is lower and EVSL is higher than the flexible charging. Thus, we can prove the introduced strategy CC to be a compromise between mobility flexibility and charging costs while exploiting BES flexibility.

For a higher user acceptance of the CC strategy, extra incentives should be required to enhance the economic benefits compared to the RC strategy. The value of  $c$  in Equation 8, which quantifies the equivalent economic benefits per hour earlier charging for different user types, could be fundamental for designing promoting mechanisms. We calculate EVSL to varying values of  $c$  and find out that EVSL is more than 90 % if  $c \geq 0.04$  € and reaches 100 % when  $c = 0.4$  €. Therefore, 0.4 € could represent the minimum compensation per hour later charging for urgent users pursuing the fastest charging under the used electricity tariff and its variation.

## Summary and future work

Within this work, we investigated user preferences concerning thermal comfort and EV charging, developed methods to quantify them, and integrated these considerations into grid-interactive BES operation strategies. The molded operation strategies were applied to a MILP formulation of a single-family house with fully electrified BES. We analyzed the resulting thermal comfort, user satisfaction regarding EV charging, electricity costs, and BES flexibility.

Comparing these factors among the BES operation strategies, our investigation showed that minimizing electricity costs per thermal comfort level could help ensure an appropriate thermal comfort level. Meanwhile, the achieved thermal comfort isn't bound with the reduction of BES flexibility and the financial benefits of a grid-interactive BES compared with other operation strategies. Thus, this operation objective could be a considerable option to promote the grid-interactive BES operation technology. The user's desire for fast charging sacrifices the BES independence in electricity supply. However, the developed charging strategy with the metric  $score_{d,t}^{EV}$  could be a good compromise between mobility flexibility, charging costs, and BES flexibility. Besides, the value of  $c$  with high EVSL quantifies the desired compensation per hour later charging of urgent drivers. This value could be fundamental for designing promotion mechanisms for intelligent grid-interactive charging behaviors.

A further step should be validating the introduced model by implementing it in more use cases. Another focus of future work could be user preferences and the owner's priorities in nonresidential buildings and their implementations in BES operation strategies.

## Acknowledgment

We gratefully acknowledge the financial support by Federal Ministry for Economic Affairs and Climate Action (BMWK), promotional reference 03EWB002A.

## References

- Ascione, F., Bianco, N., Stasio, C. de, Mauro, G.M., Vanoli, G.P., 2016. Simulation-based model predictive control by the multi-objective optimization of building energy performance and thermal comfort. *Energy and Buildings*, 111, pp. 131–144.
- aWATTar, 2021. awattar tarifblatt hourly.
- Bründlinger, T., König, J.E., Frank, O., Gründig, D., 2018. dena-Leitstudie: Integrierte energiewende. Impulse für die Gestaltung des Energiesystems bis 2050. Ergebnisbericht und Handlungsempfehlungen.
- Bundesministerium für Verkehr, Bau und Stadtentwicklung, 2007. Bekanntmachung der regeln zur datenaufnahme und datenverwendung im wohngebäudebestand, Berlin.
- Cigler, J., Prívára, S., Váňa, Z., Žáčková, E., Ferkl, L., 2012. Optimization of Predicted Mean Vote index within Model Predictive Control framework: Computationally tractable solution. *Energy and Buildings*, 52, pp. 39–49.
- Csáky, I., Kalmár, F., 2015. Effects of thermal mass, ventilation, and glazing orientation on indoor air temperature in buildings. *Journal of Building Physics*, 39 (2), pp. 189–204.
- Daina, N., Sivakumar, A., Polak, J.W., 2017. Electric vehicle charging choices: Modelling and implications for smart charging services. *Transportation Research Part C: Emerging Technologies*, 81, pp. 36–56.
- DIN 15251:2012-12, 2012. Eingangparameter für das Raumklima zur Auslegung und Bewertung der Energieeffizienz von Gebäuden – Raumluftqualität, Temperatur, Licht und Akustik. Beuth Verlag GmbH, Berlin.
- DIN 13790:2008-09, 2008. Energieeffizienz von Gebäuden - Berechnung des Energiebedarfs für Heizung und Kühlung. Beuth Verlag GmbH, Berlin.
- DIN 7730:2006-05, 2006. Ergonomie der thermischen Umgebung - Analytische Bestimmung und Interpretation der thermischen Behaglichkeit durch Berechnung des PMV- und des PPD-Indexes und Kriterien der lokalen thermischen Behaglichkeit. Beuth Verlag GmbH, Berlin.
- Jaume Salom, Joakim Widén, J Candanedo, Igor Sartori, Karsten Voss, Anna Joanna Marszal, 2011. Understanding net zero energy buildings: Evaluation of load matching and grid interaction indicators. *Building Simulation*.
- Korkas, C.D., Baldi, S., Michailidis, I., Kosmatopoulos, E.B., 2016. Occupancy-based demand response and thermal comfort optimization in microgrids with renewable energy sources and energy storage. *Applied Energy*, 163, pp. 93–104.
- Michalak, P., 2022. Thermal Network Model for an Assessment of Summer Indoor Comfort in a Naturally Ventilated Residential Building. *Energies*, 15 (10), p. 3709.
- Mohsenian-Rad, A.-H., Wong, V.W.S., Jatskevich, J., Schober, R., Leon-Garcia, A., 2010. Autonomous Demand-Side Management Based on Game-Theoretic Energy Consumption Scheduling for the Future Smart Grid. *IEEE Transactions on Smart Grid*, 1 (3), pp. 320–331.
- Oreszczyn, T., Ridley, I., Hong, S.H., Wilkinson, P., 2006. Mould and Winter Indoor Relative Humidity in Low Income Households in England. *Indoor and Built Environment*, 15 (2), pp. 125–135.
- Rauh, N., Franke, T., Krems, J.F., 2015. Understanding the impact of electric vehicle driving experience on range anxiety. *Human Factors: The Journal of the Human Factors and Ergonomics Society*, 57 (1), pp. 177–187.
- SIA 2024:2015, 2015. Raumnutzungsdaten für die Energie- und Gebäudetechnik.
- Rupp, R.F., Vásquez, N.G., Lamberts, R., 2015. A review of human thermal comfort in the built environment. *Energy and Buildings*, 105, pp. 178–205.
- Samadi, M., Fattahi, J., Schriemer, H., Erol-Kantarci, M., 2020. Demand Management for Optimized Energy Usage and Consumer Comfort Using Sequential Optimization. *Sensors*, 21 (1).
- Schütz, T., Schiffer, L., Harb, H., Fuchs, M., Müller, D., 2017. Optimal design of energy conversion units and envelopes for residential building retrofits using a comprehensive MILP model. *Applied Energy*, 185, pp. 1–15.
- van Hoof, J., 2008. Forty years of Fanger's model of thermal comfort: comfort for all? *Indoor air*, 18 (3), pp. 182–201.
- Verbruggen, B., Driesen, J., 2015. Grid Impact Indicators for Active Building Simulations. *IEEE Transactions on Sustainable Energy*, 6 (1), pp. 43–50.

- Yang, W., Zhang, G., 2009. Air movement preferences observed in naturally ventilated buildings in humid subtropical climate zone in China. *International journal of biometeorology*, 53 (6), pp. 563–573.
- Yong, J.Y., Ramachandaramurthy, V.K., Tan, K.M., Mithulananthan, N., 2015. A review on the state-of-the-art technologies of electric vehicle, its impacts and prospects. *Renewable and Sustainable Energy Reviews*, 49, pp. 365–385.
- Zhang, Q., Hu, Y., Tan, W., Li, C., Ding, Z., 2020. Dynamic Time-Of-Use Pricing Strategy for Electric Vehicle Charging Considering User Satisfaction Degree. *Applied Sciences*, 10 (9), p. 3247.